Clonality of mouse and human cardiomyogenesis in vivo

Toru Hosoda, Domenico D'Amario, Mauricio Castro Cabral-Da-Silva, Hanqiao Zheng, M. Elena Padin-Iruegas, Barbara Ogorek, João Ferreira-Martins, Saori Yasuzawa-Amano, Katsuya Amano, Noriko Ide-Iwata, Wei Cheng, Marcello Rota, Konrad Urbanek, Jan Kajstura, Piero Anversa, and Annarosa Leri[1]

Departments of Anesthesia and Medicine, and Cardiovascular Division, Brigham and Women's Hospital, Harvard Medical School, Boston, MA 02115

Edited by Darwin J. Prockop, Texas A&M Health Science Center, Temple, TX, and approved August 6, 2009 (received for review March 19, 2009)

An analysis of the clonality of cardiac progenitor cells (CPCs) and myocyte turnover in vivo requires genetic tagging of the undifferentiated cells so that the clonal marker of individual mother cells is traced in the specialized progeny. CPC niches in the atria and apex of the mouse heart were infected with a lentivirus carrying EGFP, and the destiny of the tagged cells was determined 1–5 months later. A common integration site was identified in isolated CPCs, cardiomyocytes, endothelial cells (ECs), and fibroblasts, documenting CPC self-renewal and multipotentiality and the clonal origin of the differentiated cell populations. Subsequently, the degree of EGFP-lentiviral infection of CPCs was evaluated 2–4 days after injection, and the number of myocytes expressing the reporter gene was measured 6 months later. A BrdU pulse-chasing protocol was also introduced as an additional assay for the analysis of myocyte turnover. Over a period of 6 months, each EGFP-positive CPC divided approximately eight times generating 230 cardiomyocytes; this value was consistent with the number of newly formed cells labeled by BrdU. To determine whether, human CPCs (hCPCs) are self-renewing and multipotent, these cells were transduced with the EGFP-lentivirus and injected after acute myocardial infarction in immunosuppressed rats. hCPCs, myocytes, ECs, and fibroblasts collected from the regenerated myocardium showed common viral integration sites in the human genome. Thus, our results indicate that the adult heart contains a pool of resident stem cells that regulate cardiac homeostasis and repair.

Fate mapping protocols establish a lineage relationship between ancestors carrying the reporter gene and their descendents (1, 2), but do not provide information on the self-renewing property and clonogenicity of progenitor cells or clonal origin of daughter cells in vivo (3). Because of these limitations, viral gene-tagging remains the most accurate strategy for the analysis of stem cell growth (3–8). The semi-random insertion of retroviral and lentiviral vectors represents an effective tool for genetic marking, enabling the identification of the progeny generated by stem cell differentiation. Retroviruses and lentiviruses integrate permanently in the genome of the host cells; the insertion site of the viral genome is inherited by the population derived from the parental cell (6) and can be amplified by PCR. Thus, the detection of the sites of integration constitutes a unique approach for the documentation of self-renewal, clonogenicity, and multipotentiality of stem cells in vivo. So far, this methodology has been applied to the bone marrow (4–6) and the brain (3, 7, 8) and has not been used to characterize the mechanisms regulating cardiac homeostasis and pathology.

The implementation of this technique in the adult heart is relevant for the incontrovertible demonstration of resident cardiac stem cells and the ability of the myocardium to undergo spontaneous regeneration. Moreover, the notion that cardiomyocytes have a long lifespan and their turnover is slow and age-dependent (2, 9) remains controversial (10–12). This view is not consistent with a series of reports documenting the critical role that apoptosis has in the removal of damaged myocytes and the necessary replacement of dying cells with new cardiomyocytes in animals and humans (13). The recent reconsideration of the immortal strand hypothesis of stem cell division (14), together with the need to reinterpret the long-term label retaining assay for the evaluation of stem cell growth kinetics, has required the use of complementary strategies for the measurement of cardiac cell turnover. In the current study, we have combined viral tagging with BrdU pulse-chasing in vivo to characterize the biology of c-kit-positive cardiac progenitor cells (CPCs) of the mouse and human heart (11, 15, 16).

Results

Lentiviral Tagging in Vitro. Retroviruses integrate exclusively in the genome of dividing cells (4) and may be considered the ideal tool for the selective transduction of active CPCs. However, there is one CPC per ≈40,000 cardiac cells (15, 16) and only ≈10% of CPCs are cycling in the mouse heart (11), making the possibility to infect CPCs by retroviruses unlikely. Thus, we used a lentiviral vector, which infects both cycling and noncycling cells, although lentiviruses may integrate at the same site in the genome of CPCs and myocytes that are not linearly related. However, differentiated myocytes do not divide, and our assay does not uncover insertion sites in single cells. Our protocol for the identification of proviral genome involved an inverse PCR (Fig. S1 and see *SI Methods* in *SI Appendix* for detail) and was initially tested in EGFP-labeled 3T3 fibroblasts. Different primers and restriction enzymes were used to optimize the recognition of the viral integration site. Each detected band corresponded to one insertion site as indicated by the distinct molecular weight and sequence (Fig. S2 in *SI Appendix*).

Biological Behavior of Mouse CPCs in Vivo. To characterize the pattern of CPC growth and differentiation in the mouse heart, the EGFP lentivirus was injected in proximity of the atrial and apical niches (11). The objective was to tag CPCs in situ (12) and identify the clones of differentiated cells derived from the infected CPCs (Fig. 1*A*). The recognition of a common integration site in CPCs and mature cells would reflect the clonal expansion of single CPCs and their lineage commitment. After 1–5 months, the heart was enzymatically dissociated, myocytes were separated from small cells, and EGFP-positive myocytes were identified (Fig. S3 in *SI Appendix*). Small cardiac cells were then sorted first with immunomagnetic beads and then by FACS to obtain c-kit-positive CPCs, endothelial cells (ECs), and fibroblasts (Fig. 1*B*). Vascular smooth muscle cells were not included in this analysis.

RT-PCR and immunocytochemistry were used to establish the purity of the cell preparations. Transcripts for α-myosin heavy chain (Myh6), CD31, and procollagen (Col3a1) were restricted, respectively, to myocytes, ECs, and fibroblasts (Fig. 2*A*). The expression of c-kit in these three differentiated cell populations was evaluated by nested PCR to assess the potential contamination from c-kit-

Author contributions: T.H., M.R., K.U., J.K., and A.L. designed research; T.H., D.D., M.C.C.-D.-S., H.Z., M.E.P.-I., B.O., J.F-M., S.Y.-A., K.A., N.I.-I., W.C., M.R., K.U., and J.K. performed research; T.H., J.K., P.A., and A.L. analyzed data; and T.H. and A.L. wrote the paper.

The authors declare no conflict of interest.

This article is a PNAS Direct Submission.

[1]To whom correspondence should be addressed: E-mail: aleri@partners.org.

This article contains supporting information online at www.pnas.org/cgi/content/full/0903089106/DCSupplemental.

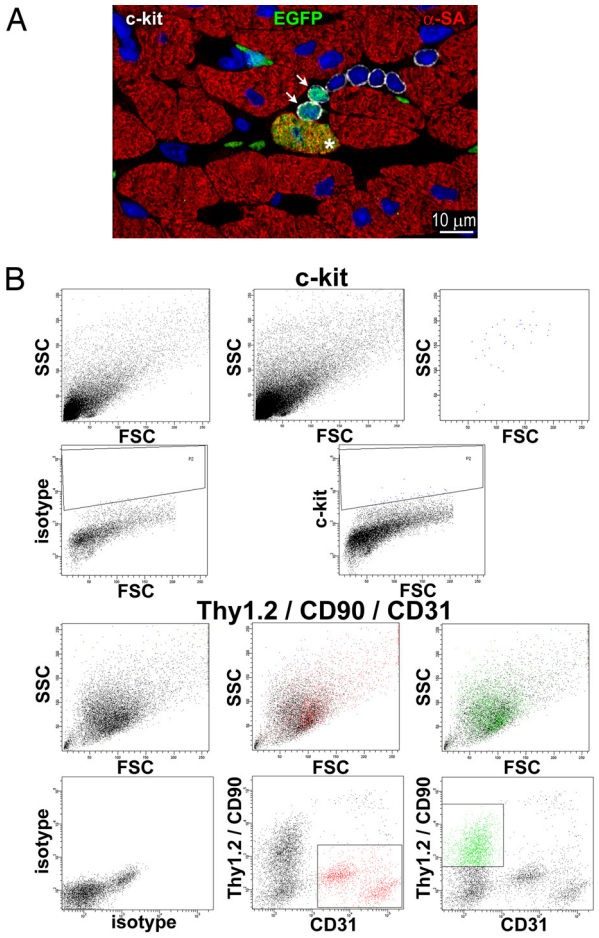

Fig. 1. Genetic tagging of CPCs in situ. (*A*) Cardiac niche containing seven CPCs (c-kit, white). Two CPCs are labeled by EGFP (green, arrows). One EGFP-positive myocyte (α-sarcomeric actin, α-SA, red) is visible (asterisk). (*B*) Scatterplots of cells co-expressing EGFP and c-kit (CPCs), EGFP and CD31 (ECs), and EGFP and Thy1.2/CD90 (fibroblasts). Forward scatter (FSC) and side scatter (SSC) are also shown. Double positive cells were back-gated and are depicted by colored dots in FSC/SSC plots.

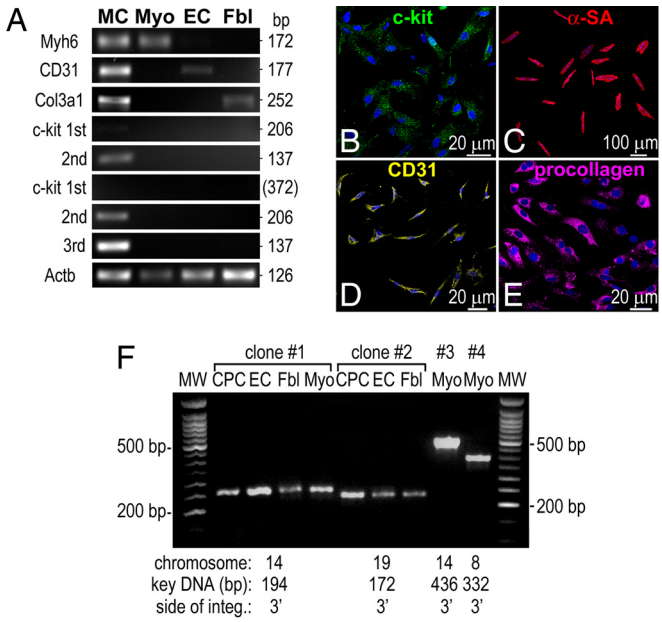

Fig. 2. Clonal marking of mouse CPCs in vivo. (*A*) Transcripts for α-MHC (Myh6), CD31 and procollagen (Col3a1) in myocytes (Myo), ECs and fibroblasts (Fbl). Transcript for c-kit were detected by two or three rounds of nested PCR. MC, mouse myocardium; Actb, β-actin. (*B–E*) FACS-sorted cardiac cells express c-kit (*B*, green), α-SA (*C*, red), CD31 (*D*, yellow), or procollagen (*E*, magenta). (*F*) Four distinct clones were identified in CPCs, ECs, Fbl, and Myo isolated from one mouse heart 4 months after EGFP-lentivirus injection. Bands of the same molecular weight correspond to identical sites of integration of the proviral sequence in the host genome. (see Fig. S4 in *SI Appendix* for clonal mapping in the mouse genome and sequences).

positive CPCs. This protocol was introduced to reach a sensitivity of detection for c-kit comparable to that used for the identification of viral integration sites; c-kit mRNA was not found in myocytes, ECs, and fibroblasts (Fig. 2*A*). Subsequently, FACS-sorted cells were plated and, after fixation, were labeled for cell type-specific antigens. c-kit, α-sarcomeric actin, von Willebrand factor, and procollagen were present only in each cell subset; these cells also retained their typical morphological appearance (Fig. 2 *B–E*).

The site of insertion of the lentiviral sequence in the mouse genome of CPCs, cardiomyocytes, ECs, and fibroblasts was detected by nested PCR. In all animals, we identified multiple PCR products (Fig. 2*F* and Fig. S4*A* in *SI Appendix*). Some of the clonal bands seen in CPCs, myocytes, ECs, and fibroblasts had the same molecular weight and a common site of integration, showing a lineage relationship between CPCs and the differentiated progeny. Our protocol does not detect viral integrants in single cells. The recognition of a unique band in CPCs indicates that a pool of these cells shared a common site of integration. This finding, together with the generation of a committed progeny, is consistent with self-renewal and clonogenicity of CPCs in vivo. Thus, the growth kinetics of CPCs corresponds to a combination of symmetric and asymmetric division, a phenomenon previously shown by the distribution of Numb and α-adaptin in the cardiac niches of the mouse heart (11). A total of 10 clones were identified in three independent experiments (Fig. S4*A* in *SI Appendix*). Based on DNA sequencing, each PCR product represented a distinct clone (Fig. S4*B* in *SI Appendix*). The presence of similar clones in different hearts reflected the semi-random integration of lentiviral vectors in the host genome (4–6).

Genomic DNA from noninfected mice was used as negative control to confirm the specificity of the assay; in all cases, no bands corresponding to viral integrants were identified (Fig. S5 in *SI Appendix*). Additionally, the actual reaction was repeated, and the same clones listed in Fig. S4 in *SI Appendix* were found (Fig. S6 in *SI Appendix*). The variability and low efficiency of self-ligation interfered with the identification of the same clones in each experiment. This limitation, apparent in Fig. S5 in *SI Appendix*, led to an underestimation of the number of clones recognized in each sample. An independent documentation of the presence of the viral integrants in cardiac cells was obtained by FISH using a digoxigenin-conjugated probe complementary to the proviral genome coding EGFP in cardiomyocytes and noncardiomyocytes (Fig. 3*A* and Fig. S7*A* in *SI Appendix*). Collectively, these results document that mature cells in the mouse heart derive from clonal activation of CPCs.

CPCs and Cardiomyogenesis. To evaluate the magnitude of myocyte progeny generated by each CPC, the EGFP lentivirus was injected in proximity of the atrial and apical niches, and the efficiency of CPC infection was measured 2–4 days later. Additionally, the absence of leakage to the mid-portion of the left ventricle (LV) was established on the premise that infected CPCs would translocate from the niches to the LV mid-region replacing dying myocytes as a result of physiological turnover. For this purpose, a group of mice was similarly treated, and the number of EGFP-positive myocytes present in the LV mid-region, distant from the sites of lentiviral delivery, was assessed 6 months later. As a complementary ap-

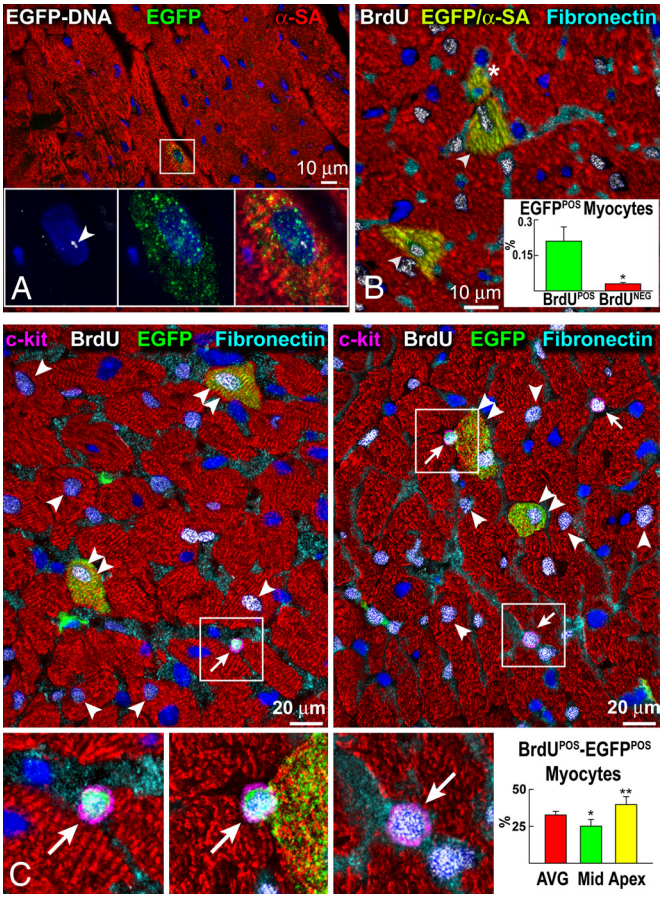

Fig. 3. CPCs and cardiomyogenesis. (*A*) FISH for EGFP viral integrants (white dot in the nucleus) found in EGFP-positive (green) myocytes (α-SA, red). Area in the rectangle is shown at higher magnification in the insets. (*B*) At 6 months, EGFP-labeled myocytes in the mid-portion of the LV are also BrdU-positive (white, arrowheads). One EGFP-positive BrdU-negative myocyte (asterisk) is visible. *, $P <$ 0.05 vs. BrdU-positive myocytes. (*C*) Most BrdU positive (white) LV myocytes do not express EGFP (arrowheads). A few BrdU-positive EGFP-positive myocytes are present (double arrowheads). CPCs express c-kit (magenta) and are labeled by BrdU (arrows). Areas in the rectangles are shown at higher magnification in the lower panels. ***, $P < 0.05$ vs. Atrioventricular groove (AVG) and mid-region (Mid), respectively.

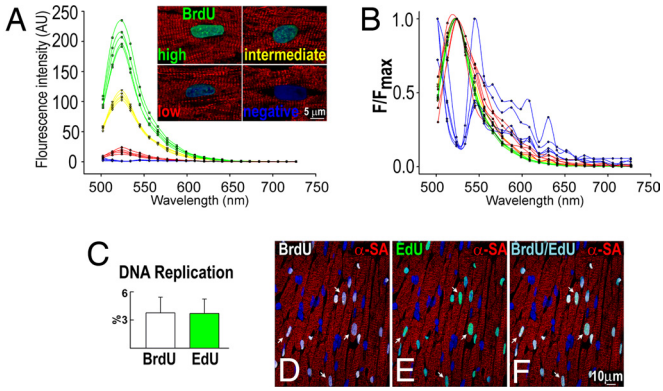

Fig. 4. Validation of BrdU labeling. (*A* and *B*) Spectral analysis of BrdU-labeled nuclei. See text for detail. (*C*) Fraction of BrdU- and EdU-labeled myocytes. (*D–F*) BrdU (white) and EdU (green) co-localize in myocyte nuclei (arrows) at the border zone of the infarct.

proach, these mice were exposed to BrdU for 3 weeks followed by a chasing period of ≈5 months. Since CPCs are slowly cycling cells and their number is low (11), a 3-weeks pulse was considered necessary for the incorporation of the BrdU in a significant fraction of primitive cells. By this protocol, the number of EGFP-positive-BrdU-positive CPCs and myocytes, and EGFP-negative-BrdU-positive CPCs and myocytes were measured to obtain information on the cumulative growth of these two cell types over a period of ≈6 months. Moreover, the number of CPCs in the atria and apex was assessed at 2–4 days and at 6 months to establish whether the CPC pool within the niches was preserved with time.

At 2–4 days, the number of EGFP-labeled CPCs per unit volume of myocardium was determined. In both regions, 14 ± 3.6 CPCs/10 mm^3 of myocardium carried the reporter gene. Also, 0.95 ± 0.30% of myocytes were EGFP-positive (Fig. S7*B* in *SI Appendix*). However, myocytes are connected to adjacent cells and do not migrate. There were no EGFP-positive cells in the LV mid-region at this time. The number of infected CPCs was small because, by design, a low titer and volume of viral suspension was administered to minimize tissue injury and prevent spreading of viral particles.

At 6 months, several EGFP-positive myocytes were identified in the LV mid-region, and these cells were almost invariably labeled by BrdU (Fig. 3*B*). The co-localization of EGFP and BrdU indicated that these myocytes were the progeny of the CPCs infected in the atrial and apical niches, which migrated to the mid-portion of the LV and differentiated. EGFP-positive CPCs were not found in this area. A small fraction of EGFP-positive-BrdU-negative myocytes were seen in the LV mid-region (Fig. 3*C*); they represented cells derived from tagged CPCs, in which BrdU reached a level of dilution that was no longer detectable. A large number of EGFP-negative-BrdU-positive myocytes were identified. These regenerated myocytes involved 33%, 25%, and 40% of the population at the atrioventricular groove (AVG), mid-region, and apex of the LV, respectively (Fig. 3*C*). At 6 months, the number of CPCs in the atria and apex was similar to that at 2–4 days (Fig. S7*C* in *SI Appendix*). These data support the notion that the heart constantly replaces old myocytes by replication and commitment of resident CPCs.

Validation of the BrdU Labeling Protocol. There is significant controversy concerning the magnitude of myocyte turnover in animals (2) and humans (9). Autofluorescence artifacts associated with BrdU labeling and other markers of cell proliferation (17) have been claimed to account for high levels of myocyte regeneration reported experimentally (11, 12) and in the human heart (10). In the current study, to validate the specificity of the recorded BrdU signals, spectral analysis was introduced to discriminate tissue autofluorescence from actual immunostaining (Fig. 4 *A* and *B*).

The emission spectra of myocyte nuclei exhibiting bright, intermediate, and dim BrdU fluorescence were obtained and compared with those of BrdU-negative nuclei (Fig. 4*A*). BrdU-positive myocyte nuclei exhibited a similar fluorescence curve with a well-defined peak at 525 nm; this corresponds to the maximum emission of FITC. When the values of the emission spectra of each curve for each nucleus were normalized by dividing the intensity of each wavelength by the peak signal, the spectra became essentially superimposable (Fig. 4*B*). Thus, all emission spectra were derived from the same fluorochrome, i.e., FITC, and the spectra acquired at different wavelengths simply reflected the amount of fluorochrome present in each nucleus. Since the emission spectra in bright, intermediate, and dim BrdU-labeled nuclei were identical, the possibility of autofluorescence was excluded. The autofluorescence signals at 525 nm wavelength was 20-fold to 200-fold lower than the intensity of the signal detected in BrdU-dim and BrdU-bright nuclei, respectively. Autofluorescence spectra lacked a well-defined maximum level and actually exhibited a trough at 525 nm.

To validate further the specificity of BrdU for the recognition of cell renewal, the thymidine analog EdU was used and compared

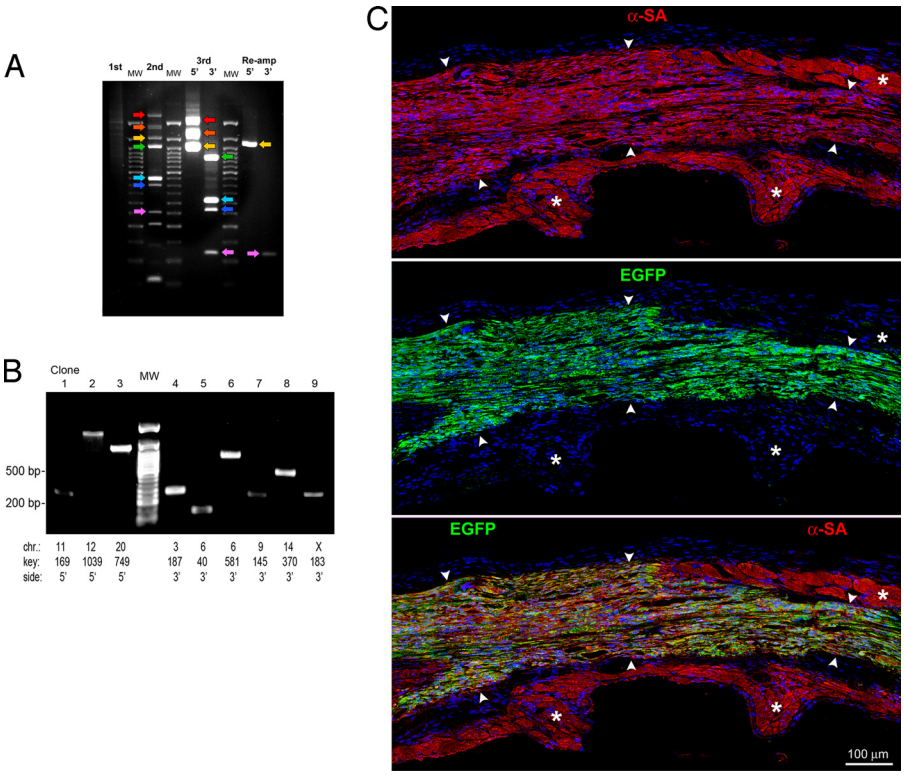

Fig. 5. Viral tagging of cultured hCPCs and myocardial regeneration. (*A*) Genomic DNA extracted from EGFP-positive-hCPCs was subjected to three rounds of PCR. The first (1st) round of PCR resulted in a DNA smear, and the second (2nd) led to the identification of seven bands. Arrows of the same color point to corresponding bands in different lanes. After the third (3rd) round, the size of the amplicons decreased by 112 bp for the 5′-side products and 138 bp for the 3′-side products. The seven bands reflect different sites of integration of the EGFP lentivirus in the human genome. PCR products were reamplified (Re-amp) and sequenced. In this example, the reamplified products of the two bands indicated by the yellow and pink arrows are shown (see Fig. S10*A* in *SI Appendix* for sequences). (*B*) Multiple clones were identified in cultured hCPCs (see Fig. S10 *B* and *C* in *SI Appendix* for chromosome mapping and sequences). (*C*) Band of regenerated myocardium (arrowheads) within the infarcted region of the LV. Newly formed myocytes express α-SA (upper panel, red) and EGFP (central panel, green). Lower panel, merge of upper and central panel. Spared myocytes (*).

with BrdU in the detection of newly formed cardiomyocytes acutely after infarction in mice. This model was introduced because acute myocardial infarction in animals and humans is characterized by activation of CPCs, and the formation of a myocyte progeny (10, 18) and BrdU has previously been used to measure myocardial regeneration after infarction in small and large mammals (15, 18), The critical aspect of this assay is that EdU is identified by click chemistry (19), which does not involve DNA denaturation and the use of an antibody, both required for the visualization of BrdU-positive cells. Additionally, click chemistry does not necessitate radioactive material and is highly reproducible (19), making it preferable and superior to autoradiography (19). Autoradiographic results are influenced by the inevitable variability in section thickness and uniform distribution of the emulsion, which interfere with resolution and condition the level of unspecific background. Quantitatively, there was a perfect correspondence between BrdU and EdU labeling of myocyte nuclei distributed in the region bordering the infarct. In animals injected with both BrdU and EdU, the two signals were concurrently detected in the same myocyte nuclei (Fig. 4 *C–F* and Fig. S8 in *SI Appendix*). Together, spectral analysis of fluorescence signals and EdU assay strongly support the technical approach and accuracy of the BrdU protocol used in this study.

Myocyte Renewal. The mid-portion of the LV contains $2.5 \pm 0.2 \times 10^6$ myocytes, and the fraction of EGFP-positive myocytes detected in this region was 0.24% (see Fig. 3*B*). Thus, ≈6,000 EGFP-positive myocytes were generated in 6 months. When this value is corrected for the efficiency of lentiviral infection of CPCs in vivo, the actual number of newly formed myocytes is 170-fold higher than that measured on the basis of EGFP labeling. As a consequence, ≈1,000,000 myocytes ($6{,}000 \times 170 = 1.0 \times 10^6$) were generated during this interval. However, according to BrdU labeling, ≈630,000 myocytes ($2.5 \times 10^6 \times 0.25 = 6.3 \times 10^5$) were formed, indicating that 25–40% of the existing parenchymal cells were replaced in 6 months in the mid-region of the LV (Fig. S9 in *SI Appendix*).

In the 10 animals analyzed at 2–4 days after lentiviral infection, an average of 26 EGFP-positive CPCs were found in each heart, indicating that ≈230 myocytes (6,000/26 = 230) were formed from each CPC over a period of 6 months (Fig. S9 in *SI Appendix*). Assuming that each CPC divided asymmetrically, the generated amplifying myocyte underwent ≈8 divisions to form this number of myocytes (≈8 divisions, each generating two cells = $2^8 = 256$ cells). The formed progeny derived from the division of amplifying myocytes, which replicate and concurrently differentiate until the adult phenotype is reached and cell cycle withdrawal is established (18). Theoretically, 26 distinct sites of integrations of the viral genome should have been detected in each heart. However, a lower number of integration sites were identified raising some questions. One possibility involves the semi-random integration of the viral DNA (4–6) in CPCs, limitations in the level of resolution of the methodology used or both. Collectively, our observations provide strong evidence in favor of the physiological import that CPCs have in the regulation of cardiac homeostasis.

Biological Behavior of Human CPCs. To determine whether, in a manner comparable to mouse CPCs, human CPCs (hCPCs) are self-renewing and multipotent, hCPCs were transduced with the EGFP-lentivirus (16). hCPCs were harvested shortly after infection, and thereby each hCPC generated a restricted number of daughter cells which inherited the maternal site of integration (Fig. 5*A* and Fig. S10*A* in *SI Appendix*). Multiple bands of different molecular weight were identified (Fig. 5*B*). Sequencing analysis showed that each band contained the proviral and human genome and reflected distinct integration sites (Fig. S10 *B* and *C* in *SI Appendix*).

Tagged hCPCs were injected shortly after coronary ligation in the region bordering the infarct. At 1 day, hCPCs engrafted and connexin 43 were detected at the interface with spared myocytes (Fig. S11*A* in *SI Appendix*). Three weeks later, an extensive portion of the infarct was replaced by a band of regenerated myocardium composed of a large number of myocytes (Fig. 5*C*), resistance arterioles, capillaries, and scattered fibroblasts (Fig. S11 *B–D* in *SI Appendix*); the new human myocytes were small and showed

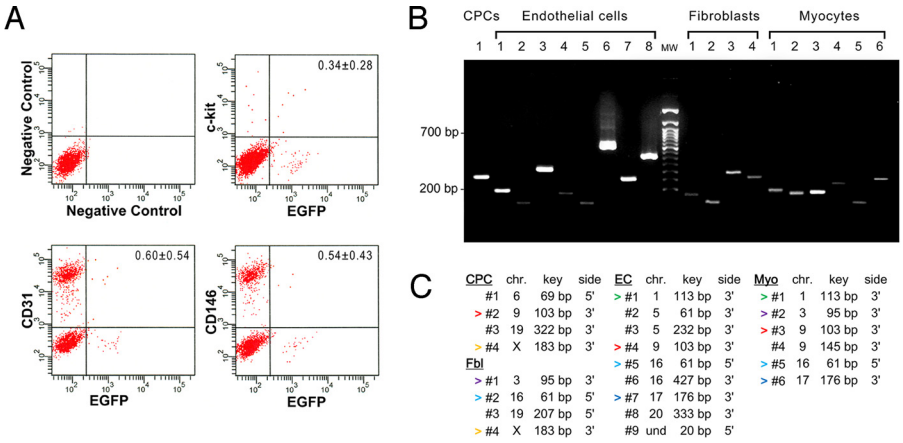

Fig. 6. Clonal tracking of hCPCs in the regenerated myocardium. (*A*) Scatterplots of EGFP-positive cells isolated from the regenerated myocardium expressing c-kit, CD31, and CD146. (*B*) Various clones were detected in distinct cardiac cell populations from the regenerated myocardium of one treated rat (see Fig. S13 in *SI Appendix* for chromosome mapping and sequences). (*C*) Sites of integration in isolated cell populations. Some clones were common to different cell classes (same color arrowheads). Key DNA sequences are ≈80 bp shorter than the corresponding clonal bands.

fetal-neonatal characteristics. However, these results did not document if individual hCPCs acquired multilineage specification in vivo or differentiated preferentially into one cell type. To establish a lineage relationship between administered hCPCs and myocardial regeneration, EGFP-positive cardiac cells were enzymatically dissociated at 4–6 weeks after infarction and cell implantation. Myocytes were separated from the small cell population, which was FACS-sorted into c-kit-positive hCPCs, ECs, and fibroblasts (Fig. 6*A*). Because of the difficulty to distinguish human fibroblasts from human ECs by the surface antigens CD146 and CD31, the identity of the sorted cells was confirmed by immunocytochemistry (Fig. S12 in *SI Appendix*).

Using primers designed for individual integration sites, we tracked each clone and its progeny, which comprised c-kit-positive hCPCs, myocytes, ECs, and fibroblasts. A total of 34 clones were identified in six independent experiments (Fig. 6*B* and Fig. S13 in *SI Appendix*). DNA sequencing showed that each PCR product with a unique band length represented distinct clones (Fig. 6*C* and Fig. S13 in *SI Appendix*). Some of the clonal bands present in hCPCs, myocytes, ECs, and fibroblasts had the same molecular weight and a common site of integration documenting a lineage relationship between hCPCs and cardiac cell lineages (Fig. 6*C*). Each random integration site represented a distinct clonal marker of the hCPC progeny that arose after cell transplantation. In one heart, four sites of integration were detected in hCPCs (Fig. 6*C*). Nested PCR was repeated, and the same clones listed in Fig. S13 in *SI Appendix* were found (Fig. S14 in *SI Appendix*). Thus, these findings support the notion of the self-renewal and multipotentiality of hCPCs and the polyclonal origin of the regenerated myocardium.

Discussion

The recognition that the heart contains a pool of progenitor cells has raised questions concerning their functional import. Several laboratories have identified CPCs in the postnatal and adult heart, their sites of storage (11, 18), their mechanisms of differentiation (18, 20, 21), and their ability to reconstitute infarcted myocardium (15, 16, 20–22). Surprisingly, the view that the heart possesses, at most, a minimal capacity to repair itself has not changed (23). Lineage tracing studies in mice have been considered the gold standard for the documentation of primitive cells in various organs and their role in the formation of a committed progeny (1, 2). However, this strategy fails to demonstrate the self-renewal and clonogenicity of progenitor cells in vivo. Similarly, the presence of the reporter gene in mature cells cannot be attributed to a single founder cell leaving unanswered the question concerning the multipotentiality of stem cells (3). These problems have been addressed in the current study in which viral transduction for clonal tracking of individual mouse and human CPCs was used to determine their fate physiologically and after injury in vivo.

Genetic tagging with retroviruses was introduced more than 20 years ago (24) for the in vivo characterization of the multipotentiality of hematopoietic stem cells (HSCs). Differentiation assays of stem cell clones in vitro have inherent limitations including the possibility that culture protocols result in the preferential acquisition of a selective lineage phenotype, masking the full potential of the founder cell. Similarly, the identification of multiple cell types in the progeny of transplanted nonclonogenic stem cells does not provide direct evidence of the multipotentiality of each delivered cell. These problems have been overcome with viral clonal marking, which was designed for the analysis of bone marrow HSCs and derived blood cells (4–6, 24). Retrovirus-mediated fate tracing and BrdU labeling have been used in an attempt to characterize the multipotentiality of neural stem cells in the adult mouse hippocampus and subventricular zone (3, 7).

Viral tagging cannot be applied to solid organs such as the heart without caveats. Limitations involve the low efficiency of CPC infection and the impossibility to collect serial samples of the transduced progeny in small animals. Moreover, whether the insertion site confers a selective advantage or disadvantage to the growth of single cells may be easily assessed in blood cells (5) but cannot be established in the heart. The restricted number of infected cells in the current study has precluded the transplantation of transduced CPCs in secondary and tertiary recipients. This would represent the ideal methodology for the documentation of CPC self-renewal. However, the preservation of the pool of CPCs in the atrial and apical niches over a period of 6 months strongly suggests that these cells retained their self-renewal ability and divided.

EGFP is a widely used reporter gene for the analysis of the fate of progenitor cells in vivo. However, the immunogenic potential of this foreign protein has raised questions on the appropriateness of its utilization in long-term studies. Processed peptides derived from EGFP may be presented by the major histocompatibility complex on the cell surface, inducing a T cell immune response against the labeled cells (25). The magnitude of immunological rejection of cells carrying EGFP remains controversial and most likely context-dependent (25). Whether this phenomenon is operative in our system remains to be determined. We may have underestimated the number of EGFP-positive CPCs and myocytes present at 6 months after lentiviral infection. An additional variable that may have influenced the assessment of myocyte formation from CPCs involves the insertion of the proviral integrant in repressive regions of the mouse genome (26). However, transgene silencing interferes with the recognition of labeled cells by immunocytochemistry but does not affect the analysis of integration sites by PCR.

As in the brain (3, 7), the two markers of cardiomyogenesis introduced here, EGFP integration in the mouse genome and BrdU

labeling, indicate that activation and differentiation of CPCs is an ongoing process that results in a significant turnover of cardiomyocytes in the young-adult mouse heart. This phenomenon increases with chronological age in the heart to compensate for the progressive increase in myocyte death in old animals (12) and humans (27). However, enhanced cell regeneration does not counteract ongoing cell death in the myocardium, resulting in a decreased number of parenchymal cells in the senescent heart. An imbalance between cell death and regeneration with aging has also been observed in other organs including the brain, the bone marrow, the liver, the pancreas, and skin melanocytes (28).

Our observations are consistent with the notion that cardiac homeostasis is regulated by a compartment of resident CPCs and support the view that, albeit inadequate, myocyte formation is a relevant component of myocardial regeneration in the overloaded heart. The high level of myocyte turnover documented by viral tagging and BrdU labeling is at variance with fate mapping studies (2) and other analyses of DNA synthesis (17), suggesting that very little replacement, if any, of myocytes occurs with age. An opposite phenomenon has recently been claimed using the incorporation of ^{14}C in the human heart, in which myocyte renewal was found to be mostly restricted to young individuals being dramatically reduced in old pathologic hearts with untreated hypertension, hypertrophy, and myocardial infarction (9). Thus, ^{14}C retrospective birth dating of human cardiomyocytes contradicts the lineage tracing study in the mouse and previous reports showing significant degrees of cycling amplifying myocytes, high myocyte mitotic index, and increased myocyte number after myocardial infarction or hypertensive hypertrophy in the elderly (10, 29). The ^{14}C labeling strategy was conducted in myocyte nuclei expressing the contractile protein troponin I (TnI). The localization of TnI in nuclei is surprising and may coincide with a peculiar functional state of a restricted pool of cells and may not be representative of the entire myocyte population.

The absence of myocyte turnover postulated in the mouse heart up to 1 year of age (2) is inconsistent with the magnitude of cell death identified in the aging mouse myocardium. The young adult mouse heart typically shows a degree of myocyte apoptosis of ≈300 cells per million or one-thirtieth of 1% (30). Although this may be seen as inconsequential physiologically, the duration of this form of cell death is at most 4 h. Thus, ≈1,800 myocytes/10^6 cells are lost per day in the heart. Since there are 3.4 million myocytes in the mouse LV, ≈6,100 cells die per day in the entire LV. Over a period of 6 months, ≈1.1 million myocytes would be lost and have to be replaced by new cells to preserve cardiac function. Also, in tracing studies, the use of tamoxifen to activate Cre-recombinase has negative effects on the structure and function of the heart, resulting in a transient dilated cardiomyopathy (31), which may affect the evolution of the aging heart (2). Leakage of the transgene and the impossibility to discriminate the rate of turnover in one-fifth of the myocyte population that does not respond to tamoxifen (2) further confound the interpretation of fate mapping results raising questions on the conclusions reached on myocyte turnover by this genetic strategy.

In conclusion, genetic marking of CPCs in situ has provided the opportunity to assess the behavior of tissue-resident CPCs in the noninjured heart. Although the extent of myocyte turnover in the intact heart is slower than the rapid pace at which cells renew themselves in the presence of damage, the intrinsic properties of CPCs are better characterized when tissue lesions are absent. A critical question is whether cardiac repair after injury recapitulates the developmental steps of CPC lineage commitment in the organ in a steady state in which the invariant growth mechanism preserves the stem cell pool and produces an adequate progeny. The present study has also acquired information concerning the multipotentiality of hCPCs and the polyclonal origin of myocardial regeneration after infarction. A strategy has been developed for the evaluation of the in vivo behavior and function of stem cells delivered to the heart. By this approach, clinically relevant questions of cell therapy for the failing heart may be addressed, including the clonal heterogeneity of hCPCs and the repopulation properties of individual cells. The acquisition of positive results has strengthened the possibility that hCPCs may have implications for the management of human heart failure.

Methods

Viral Integration Sites. Mice at 3 months of age were injected at the AVG and apex with a lentivirus encoding EGFP (15). At 1–5 months, genomic DNA was collected separately from myocytes, CPCs, ECs, and fibroblasts, and a newly developed PCR-based methodology (AKANE) was performed. A similar analysis was conducted in EGFP-hCPCs injected in the border zone of infarcted immunosuppressed rats (20). Detailed methods are found in *SI Appendix*.

ACKNOWLEDGMENTS. This work was supported by grants from the National Institutes of Health. J.F.-M. was supported by the Foundation for Science and Technology, Ministry of Science, Technology and Higher Education, Portugal.

1. Barker N, et al. (2007) Identification of stem cells in small intestine and colon by marker gene Lgr5. *Nature* 449:1003–1007.
2. Hsieh PC, et al. (2007) Evidence from a genetic fate-mapping study that stem cells refresh adult mammalian cardiomyocytes after injury. *Nat Med* 13:970–974.
3. Suh H, et al. (2007) In vivo fate analysis reveals the multipotent and self-renewal capacities of Sox2+ neural stem cells in the adult hippocampus. *Cell Stem Cell* 1:515–528.
4. Schmidt M, et al. (2003) Clonality analysis after retroviral-mediated gene transfer to CD34+ cells from the cord blood of ADA-deficient SCID neonates. *Nat Med* 9:463–468.
5. Mazurier F, Gan OI, McKenzie JL, Doedens M, Dick JE (2004) Lentivector-mediated clonal tracking reveals intrinsic heterogeneity in the human hematopoietic stem cell compartment and culture-induced stem cell impairment. *Blood* 103:545–552.
6. Dunbar CE (2005) Stem cell gene transfer: Insights into integration and hematopoiesis from primate genetic marking studies. *Ann NY Acad Sci* 1044:178–182.
7. Seri B, et al. (2006) Composition and organization of the SCZ: A large germinal layer containing neural stem cells in the adult mammalian brain. *Cereb Cortex* 1:i103–i111.
8. Rompani SB, Cepko CL (2008) Retinal progenitor cells can produce restricted subsets of horizontal cells. *Proc Natl Acad Sci USA* 105:192–197.
9. Bergmann O, et al. (2009) Evidence for cardiomyocyte renewal in humans. *Science* 324:98–102.
10. Beltrami AP, et al. (2001) Evidence that human cardiac myocytes divide after myocardial infarction. *N Engl J Med* 344:1750–1757.
11. Urbanek K, et al. (2006) Stem cell niches in the adult mouse heart. *Proc Natl Acad Sci USA* 103:9226–9231.
12. Gonzalez A, et al. (2008) Activation of cardiac progenitor cells reverses the failing heart senescent phenotype and prolongs lifespan. *Circ Res* 102:597–606.
13. Yaoita H, Maruyama Y (2008) Intervention for apoptosis in cardiomyopathy. *Heart Fail Rev* 13:181–191.
14. Rando TA (2007) The immortal strand hypothesis: Segregation and reconstruction. *Cell* 129:1239–1243.
15. Beltrami AP, et al. (2003) Adult cardiac stem cells are multipotent and support myocardial regeneration. *Cell* 114:763–776.
16. Bearzi C, et al. (2007) Human cardiac stem cells. *Proc Natl Acad Sci USA* 104:14068–14073.
17. Rubart M, Field LJ (2006) Cardiac regeneration: Repopulating the heart. *Annu Rev Physiol* 68:29–49.
18. Boni A, et al. (2008) Notch1 regulates the fate of cardiac progenitor cells. *Proc Natl Acad Sci USA* 105:15529–15534.
19. Buck SB, et al. (2008) Detection of S-phase cell cycle progression using EdU incorporation with click chemistry, an alternative to using BrdU antibodies. *Biotechniques* 44:927–929.
20. Martin CM, et al. (2008) Hypoxia-inducible factor-2alpha transactivates Abcg2 and promotes cytoprotection in cardiac side population cells. *Circ Res* 102:1075–1081.
21. Pfister O, et al. (2008) Role of the ATP-binding cassette transporter Abcg2 in the phenotype and function of cardiac side population cells. *Circ Res* 103:825–835.
22. Smith RR, et al. (2007) Regenerative potential of cardiosphere-derived cells expanded from percutaneous endomyocardial biopsy specimens. *Circulation* 115:896–908.
23. Parmacek MS, Epstein JA (2009) Cardiomyocyte renewal. *N Engl J Med* 361:86–88.
24. Lemischka IR, Raulet DH, Mulligan RC (1986) Developmental potential and dynamic behavior of hematopoietic stem cells. *Cell* 45:917–927.
25. Stripecke R, et al. (1999) Immune response to green fluorescent protein: Implications for gene therapy. *Gene Ther* 6:1305–1312.
26. Stewart R, et al. (2008) Silencing of the expression of pluripotent driven-reporter genes stably transfected into human pluripotent cells. *Regen Med* 3:505–522.
27. Chimenti C, et al. (2003) Senescence and death of primitive cells and myocytes lead to premature cardiac aging and heart failure. *Circ Res* 93:604–613.
28. Sharpless NE, DePinho RA (2007) How stem cells age and why this makes us grow old. *Nat Rev Mol Cell Biol* 8:703–713.
29. Olivetti G, et al. (1994) Myocyte nuclear and possible cellular hyperplasia contribute to ventricular remodeling in the hypertrophic senescent heart in humans. *J Am Coll Cardiol* 24:140–149.
30. Odashima M, et al. (2007) Inhibition of endogenous Mstl prevents apoptosis and cardiac dysfunction without affecting cardiac hypertrophy after myocardial infarction. *Circ Res* 100:1344–1352.
31. Molkentin JD, Robbins J (2009) With great power comes great responsibility: Using mouse genetics to study cardiac hypertrophy and failure. *J Mol Cell Cardiol* 46:130–136.